DOI: https://doi.org/10.1021/acssuschemeng.6b02796

Article

High-performance magnetic activated carbon from solid waste from lignin conversion processes. Part II: Their use as NiMo catalyst supports for lignin conversion.

Mikel Oregui-Bengeochea, Nemanja Mileti#, Wenming Hao, Fredrik Björnerbäck, Mali Husby Rosnes, Jose Javier Saiz Garitaonandia, Niklas Hedin, Pedro L. Arias, and Tanja Barth

ACS Sustainable Chem. Eng., **Just Accepted Manuscript** • DOI: 10.1021/acssuschemeng.6b02796 • Publication Date (Web): 13 Oct 2017

High-performance magnetic activated carbon from solid waste from lignin conversion processes. Part II: Their use as NiMo catalyst supports for lignin conversion.

Mikel Oregui-Bengoechea*[a] (mikel.oregui@ehu.eus), Nemanja Miletić[b,c] (n.m.miletic@gmail.com), Wenming Hao[d,e] (wenminghao9@gmail.com), Fredrik Björnerbäck[d,e] (fredrik.bjornerback@mmk.su.se), Mali H. Rosnes[a] (Mali.Rosnes@uib.no), J. S. Garitaonandia[f] (js.garitaonandia@ehu.es), Niklas Hedin[d,e] (niklas.hedin@mmk.su.se), Pedro L. Arias[b] (pedroluis.arias@ehu.es) and Tanja Barth[a] (Tanja.Barth@uib.no)

[a] Department of Chemistry, University of Bergen, Allégaten 41, 5007 Bergen, Norway

[b] Department of Chemical and Environmental Engineering, School of Engineering, University of the Basque Country (EHU/UPV), C/Alameda Urquijo s/n,48013 Bilbao, Spain

[c] Department of Food Technology, Faculty of Agronomy, University of Kragujevac, Cara Dušana 34, 32000 Čačak, Serbia

[d] Department of Materials and Environmental Chemistry, Arrhenius Laboratory, Stockholm University, SE-106 91 Stockholm, Sweden

[e] Berzelii Center EXSELENT on Porous Materials, Arrhenius Laboratory, Stockholm University, SE-106 91 Stockholm, Sweden

[f] Fisika Aplikatua II Saila, Euskal Herriko Unibertsitatea, 644 P. K. 48080 Bilbao, Spain

Keywords: Lignin catalytic conversion, formic acid, hydrodeoxygenation (HDO), magnetic activated carbons, NiFe

SYNOPSIS

Large quantities of low-value hydrochar are typically produced in lignin conversion processes. In this paper, hydrochar is valorized into activated carbon and re-used as catalyst support in the same process.

ABSTRACT

Lignin conversion processes produce carbon rich residues[1,2] that can be converted into valuable materials such as magnetic activated carbons (MACs). Such lignin-derived MACs can be further used as functional substrates for hydrotreating NiMo catalysts. In this work, we studied the activity of different NiMo-MACs for the catalytic conversion of lignin in a formic acid/ethanol media (LtL process). Two KOH-activated LtL hydrochars from Eucalyptus (MACE) and Norwegian Spruce (MACS) lignins were used as catalyst supports. In addition, the activity of the resulting NiMo-MACs, namely C-MACE and C-MACS, was compared with a NiMo catalyst supported on a commercial activated carbon (AC). At reaction conditions of 340 °C and 6 h, the best result was obtained for the NiMo-MACS with a yield of 72.2 wt.% of oil and 21.1 wt.% of organic solids. At 300 °C and 10 h, both NiMo-MAC catalysts displayed higher HDO activities than their commercial counterpart, yielding considerably higher oil yields. The higher HDO activities are tentatively assigned to the formation of NiFe species on the catalytic surfaces of the NiMo-MAC catalysts. In addition, the magnetism exhibited by the C-MACS made it easy to recover the catalyst. However, a considerable loss of activity was observed upon recycling due to a chemical modification of the catalyst surface.

INTRODUCTION

In a biorefinery, biomass conversion processes and technologies are integrated to produce fuels and value-added chemicals and products[2,3]. When developing sustainable and economically efficient bio-refinery concepts, it is especially interesting to study unexploited biomass resources and wastes, and their conversion into bio-oils and/or value-added products[4]. Lignin is a major byproduct from the pulp-and-paper industry and from biomass pretreatment processes for bio-ethanol production[5,6]. This natural amorphous polymer can be thermochemically converted into bio-oil and fine chemicals[7,8], although in most cases there are side reactions that convert a considerable amount of the biopolymer into organic solids or hydrochar[2,9–11].

A promising and relatively new approach to convert lignin, known as lignin-to-liquid (LtL), involves the use of formic acid (FA) together with a solvent, either ethanol or water. High oil yields, with high H/C and low O/C ratios, are obtained, whilst retaining the phenol-type structure of the bio-oil components. Nevertheless, high temperatures (typically 350-400 °C) and long reactions times (typically 8-16 h) are needed to convert the lignin feedstock into bio-oil in high yields[12,13]. Thus, in order to produce fuels and chemicals that can compete with traditional petroleum based products, two main issues need to be addressed: lowering the process severity (temperature and reaction time), and valorizing the low-value side streams. Such side streams include solid residues/hydrochars that can be further processed into value-added products.

Two different strategies can be used to enhance the competitiveness of the LtL process. The reaction rates can be increased by using a catalyst and/or the hydrochar byproducts can be further processed into valuable products. With a suitable catalyst, the lignin de-polymerization and hydrodeoxygenation (HDO) rates for producing the target aromatic compounds could be improved. In this context, several combinations of traditional hydrotreating catalysts have been

extensively studied, and their activities for thermo-catalytic conversion of lignin into bio-oil have been proven. Typical examples of such catalysts are NiMo-based sulfided catalysts and noble metals (Rh, Ru, Pd, Pt) over a wide variety of supports (i.e. alumina, silica, zeolites, activated carbon and zirconia)[2,14–16]. However, sulfided catalysts require a continuous addition of H_2S to remain stable and active, making them less suited for lignin HDO due to the risk of sulfur incorporation in the bio-oil products[17]. Noble metals are not the preferred choice as their large ring hydrogenation selectivity decreases the content of aromatic products of the bio-oil increasing the amount of saturated alcohols instead. Furthermore, their cost may make them less relevant for industrial production of lignin-derived aromatics[18]. Regarding the support, HDO catalyst supported on activated carbons (ACs) are promising alternatives to traditional metal oxide supported catalysts due to (i) less coking[19,20] (ii) low cost and (iii) the possibility of recovering the active metals from spent catalysts by burning off the carbon. Moreover, the textural and surface chemical properties of ACs might be tailored by varying the activation procedure[21].

The second approach to increase the competitiveness of the LtL process is to convert the solid organic residues to functional carbon materials. Several groups have studied the conversion of lignin and other biomass sources into renewable ACs for various purposes[7,22–28]. To our knowledge, except for a previous joint study[29], no previous research been performed to convert solid organic residues of LtL processes (or other lignin processing related solid residues) into functional carbon materials such as ACs. In that study, we activated such residues into magnetic activated carbons (MACs) with high surface areas and studied their potential use in CO_2 separation.

Here, we studied these lignin-derived and iron-containing MACs as catalyst supports for non-sulfided NiMo catalysts in the LtL conversion process. The activity of these NiMo-MACs

was studied and compared with a NiMo catalyst supported on a conventional AC. The observed increases in the oil yields and decreases in the solid yields were compared to the non-catalyzed system (NC) and used as the primary evaluation parameters. The catalytic effect of the supports alone and the influence of pre-reducing the catalysts on the LtL conversion yields were also investigated. The promoting effects of Fe on the NiMo/MACs catalysts were also evaluated and discussed. Finally, the stability of the C-MACS catalyst upon recycling was determined.

EXPERIMENTAL SECTION

Chemicals

Formic acid (>98%), tetrahydrofuran (THF) (>99.9%), ethyl acetate (EtAc) (99.8%), hexadecane (>99.8 %) and anhydrous sodium sulphate (>99.0 %) were purchased from Sigma Aldrich and used as supplied. Nickel(II) nitrate hexahydrate (99.9+% Ni), ammonium molybdate tetrahydrate (99.98% Mo) and a commercial AC were purchased from Strem Chemicals Inc.

Rice straw lignin from strong acid carbohydrate dissolution pre-treatment was received from Technical College of Bergen. The lignin was ground, and sieved (<500 μm) prior to use. This lignin contained 14.9 wt. % of inorganic components as determined following the procedure described in the *Supporting Information* (Table S1).

Synthesis of the catalyst

Three types of supports were used:

(i) A commercial AC, which was used as received; this AC had a negligible content of Fe; (ii) A MAC produced from eucalyptus-lignin hydrochar (MACE). This AC contained a significant Fe concentration and exhibited ferromagnetic properties. The experimental procedures used for the synthesis and activation of the hydrochar are described elsewhere[29]. In that study, the name was somewhat longer, MAC-E-8, to specify the temperature of activation (800°C)[29]. This MACE support was used as received. (iii) A MAC produced from Norwegian spruce-lignin hydrochar (MACS). This AC also contained a significant Fe concentration and exhibited ferromagnetic properties. The experimental procedures used for the synthesis and activation of the hydrochar are described elsewhere[29]. In that study, the name was somewhat longer, MAC-S-7, to specify the temperature of activation (700°C). This MACS support was used as received.

The corresponding catalysts were prepared by successive wet impregnation (WI). The supports were first mixed with deionized water in a 1:5 weight ratio, after which ammonium molybdate ($(NH_4)_6Mo_7O_{24}\cdot 4H_2O$)) was added. The solutions were stirred overnight. Excess of solvent was removed by heating at 60 °C under dynamic vacuum, and samples were subsequently dried in a furnace at 105 °C for 20 min. The resulting solids were impregnated with nickel (II) nitrate hexahydrate ($Ni(NO_3)_2\cdot 6H_2O$) following the same procedure. The nominal MoO_3 and NiO loadings of the catalysts were 12 wt.% and 5 wt.%, respectively. The solids were calcined under a flow of N_2 (10 mL/min) at 470 °C for 2 h using a heating ramp of 2 °C/min, and named C- AC, C- MACE and C- MACS. Finally, the calcined catalysts were subjected to another thermal treatment in a H_2/N_2 (10/90, vol/vol) flow (10 mL/min) at 450 °C for 2 h with a heating ramp of 2 °C/min. The resulting pre-reduced catalysts were named H- AC, H- MACE and H- MACS and used shortly after the treatment.

Two additional calcined catalyst were synthesized to evaluate the effect of the type of support and its acidity. These catalysts were based on metal oxide supports: a NiMo catalyst supported on a Lewis solid acid, i.e. Al_2O_3, and a NiMo catalyst supported on a non-acidic support, i.e. ZrO_2. The catalysts were named C-Al_2O_3 and C-ZrO_2. The synthesis procedure was equivalent to the one described for the C-AC, C-MACE and C-MACS catalysts, except that they were calcined in air.

The catalysts were characterized by N_2-adsorption, inductively coupled plasma atomic emission spectroscopy (ICP-AES), X-ray diffraction (XRD) and Mössbauer spectroscopy following the procedures described in the *Supporting Information*.

Catalytic conversion of lignin in a formic acid/ethanol media (LtL experiments)

Experimental set-up: Rice straw lignin (2 g), formic acid (1.5 g), ethanol (2.5 g) and the catalyst (0.2 g) were added to a stainless steel reactor (Parr 4742 non-stirred reactor, 25 mL volume). The reactor was closed and heated in a Carbolite^{TM} LHT oven to 300-340°C for 2, 6 or 10 h. Two replicates were performed for each experiment, and the results refer to the related average. For the non-catalyzed (NC) experiments, the oil and solid yield values differed more than 3.0 wt. % units relative to the lignin input; thus additional experiments were carried out until the difference was less than 3.0 wt. %. The amount and concentration for each reactant is summarized in the *Supporting Information* (Table S2). The experiments are named after the type of catalyst used and the reaction conditions.

Work-up procedure: After the reaction, the reactor was removed from the oven and cooled to ambient temperature by natural convection. The amount of produced gases was determined by weighing the reactor before and after ventilating the gas. The reactor was opened and the liquid reaction mixture was extracted with a solution of ethyl acetate EtAc:THF (90:10). The solid phase (unreacted lignin, inorganic and organic lignin residues and catalyst) was filtered off. The dark-brown organic liquid phase was dried over anhydrous Na_2SO_4 and concentrated at a reduced pressure of 160 mbar and a temperature of 40°C to eliminate the remaining EtAc:THF and the ethanol. The final oil and solid yields were determined by weight (amount of oil or solids (g)/amount of introduced lignin (g)) after the work-up procedure was completed. The solid yield for the catalyzed systems was calculated after subtracting the amount of catalyst introduced, hence, the solid yield referred to the sum of the organic solids (hydrochar) and the inorganic lignin ashes. The oil was characterized by elemental analysis, GC-MS and GPC-SEC following the experimental procedures described in the *Supporting Information*.

Recyclability of the catalyst: The activity of the C-MACS catalyst was evaluated upon recycling at two different reaction conditions: 340°C and 6 h and at 300°C and 10 h. Three consecutive tests were carried out at each reaction condition: (i) with the fresh C-MACS catalysts (the C-MACS-340-6 and C-MACS-

300-10 experiments); (ii) with the recycled catalysts from the test (i), (the R1-MACS-340-6 and R1-CMACS-300-10 experiments), and (iii) with the recycled catalysts from test (ii) (the R2-MACS-340-6 and R2-CMACS-300-10 experiments). The catalysts were recovered as follows: after each test the solid phase (catalysts, inorganic solids and hydrochar) were washed with a solution of EtAc:THF (90:10) for 24 h in a Soxhlet unit to remove the soluble organic components, leaving a solid residue. Later the catalyst was separated from the residual lignin solids (inorganic solids and hydrochar) with the aid of a niobium magnet and re-used in the LtL process. In the case of test (iii), the low magnetization of the catalyst only allowed recovering enough catalyst to carry out a single replicate (experiments R2-MACS-340-6 and R2-MACE-300-10). The amount and concentration for each reactant is summarized in the *Supporting Information* (Table S2).

The recycled catalysts were characterized by N_2-adsorption, inductively coupled plasma atomic emission spectroscopy (ICP-AES), X-ray diffraction (XRD) and scanning electron microscopy and energy dispersive X-ray (SEM-EDX), following the procedures described in the *Supporting Information*.

RESULTS

Catalyst characterization

In the previously reported study[29], we derived MACs from the LtL hydrochars of eucalyptus and Norwegian spruce, and studied them as potential CO_2 adsorbents. Their composition and magnetic, textural and morphological properties were also thoroughly analyzed.

Here, we have synthesized and tested NiMo-based catalysts supported on these MACs in the LtL conversion. The main characteristics of the AC, MACE and MACS and their respective NiMo-based catalysts (calcined under N_2 atmosphere and pre-reduced) are summarized in Table 1.

N_2-adsorption: The textural properties of the bare supports varied depending on the nature and activation process. The adsorption-desorption isotherm and the pore size distribution for the commercial AC in Figure 1a and Figure 1d, suggested a mainly microporous nature but with some mesopores with sizes 2 – 4 nm. The BET surface area of the AC was 1415 m^2/g and its total pore volume (V_t) was 0.92 cm^3/g (Table 1). The textural properties of the MACE and MACS are presented elsewhere[29]. Briefly summarized, MACE contained both micropores and small size mesopores (between 2 – 4 nm), while MACS contained only micropores. MACE and MACS had BET surface areas and total pore volumes of 2875 m^2/g and 0.92 cm^3/g, and of 1380 m^2/g and 0.62 cm^3/g, respectively.

Table 1: Textural properties, metal content and Ni dispersion of commercial activated carbon (AC), magnetic activated carbon (MACE and MACS) the NiMo-based catalysts

Catalyst (A[a] - B[b])	S_{BET} (m^2/g)	V_t (cm^3/g)	ICP-AES		
			Ni (wt%)	Mo (wt%)	Fe (wt%)
AC	1415	0.92	-[d]	-[d]	-[d]
MACE	2875[c]	1.59[c]	-[d]	-[d]	6.4[c]
MACS	1380[c]	0.62[c]	-[d]	-[d]	12.25[c]
C-AC	1258	0.68	3.7	7.5	0.6
C-MACE	2263	1.24	4.8	7.8	6.1
C-MACS	1189	0.57	5.2	7.8	17.6
H-AC	1037	0.84	-[d]	-[d]	-[d]
H-MACE	2268	1.29	-[d]	-[d]	-[d]
H-MACS	1061	0.54	-[d]	-[d]	-[d]

[a] A: refers to the type of systems: bare support (none), NiMo containing calcined catalyst (C), NiMo containing pre-reduced catalyst (H) [b] B: refers to the type of support: AC, MACE and MACS [c] These values were reported in a previous joint study[29] [d] The analysis were not carried out

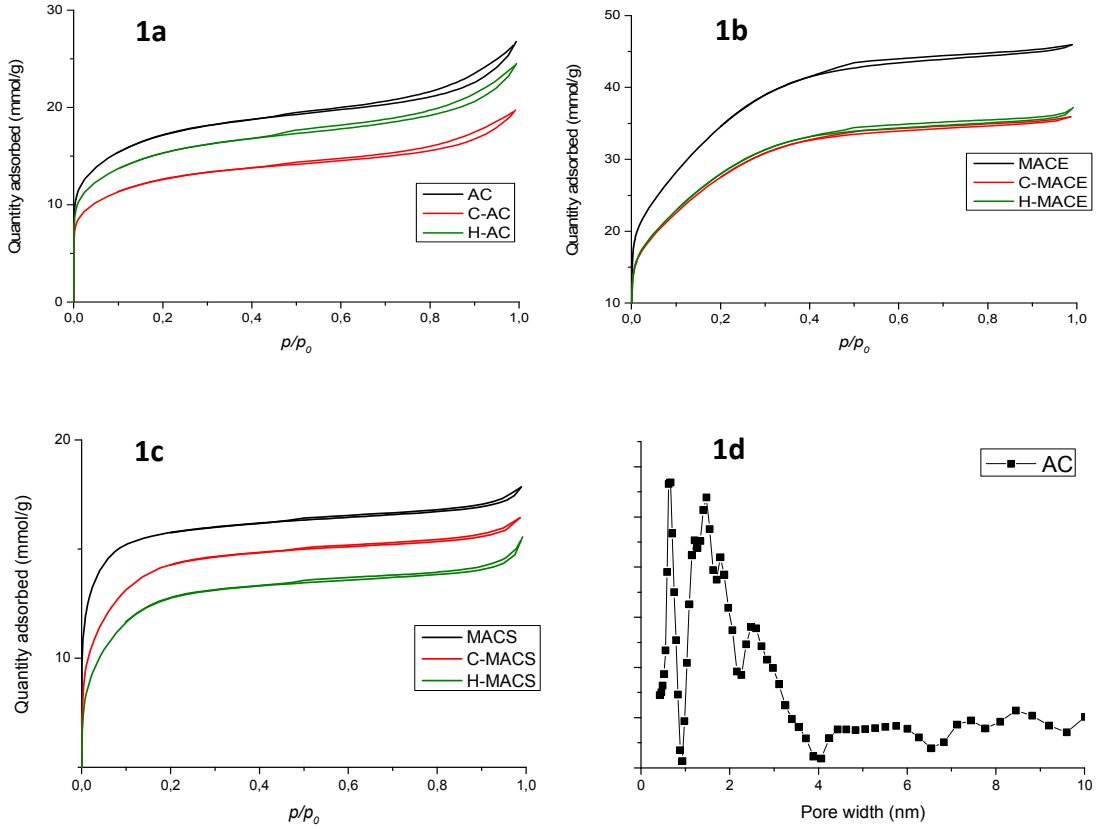

Figure 1. N_2 adsorption-desorption isotherms for: (a) AC (black), C-AC (red) and H-AC (green); (b) MACE (black), C-MACE (red) and H-MACE (green); (c) MACS (black), C-MACS (red) and H-MACS (green). MAC denotes magnetic activated carbon, C-X NiMo containing calcined catalyst and support, H-X NiMo containing pre-reduced catalyst. The N_2 isotherms for MACE and MACS are reported elsewhere[29] (d) pore size distribution for the AC carbon using DFT model

The surface areas were reduced upon supporting Ni and Mo in all cases (Table 1 and Figure 1. The decreases were accompanied by decreasing total pore volumes, which indicated that the reduced surface areas were due to partial blockage of the pores by Ni and Mo species. The effect on the textural properties of pre-reducing the samples depended on the type of support

(Table 1 and Figure 1). In the case of the MACE, an insignificant increase in the surface area was observed, while the surface areas decreased for the H-AC and H-MACS catalyst.

ICP-AES: Elemental analyses of Ni, Mo and Fe were carried out only for the C-series catalysts. The C-MACE catalysts had an Fe content of 6.1 wt.%, while the Fe content of the C-MACS catalyst was considerably higher, 17.6 wt.%. The C-AC, on the other hand, contained a negligible content of Fe, 0.6 wt.%. These trends confirmed that the high content of Fe in C-MACE and C-MACS could be attributed to the content of Fe in their parent MACs.

In addition, the C-MACE and C-MACS contained a higher amount of Ni in comparison to the C-AC: the C-MACE and C-MACS contained 4.8 wt. % and 5.2 wt. % of Ni, while the C-AC only 3.7 wt. %. The content of Mo, however, was comparable in all cases: 7.5 wt. % for the C-AC, and 7.8 wt. % for both C-MACE and C-MACS.

X-ray diffraction (XRD): The XRD diffractograms of the C-AC, H-AC, C-MACE, H-MACE, C-MACS, and H-MACS are shown in Figure 2. Intense graphitized carbon peaks were detected in the C-AC, and H-AC, with characteristic reflections at 2θ angles of 26.6° and 43.8° (carbon, PDF: 00-026-1080). Graphitized carbon was also detected in the MACE and MACS samples, although their XRD reflection intensities were significantly smaller.

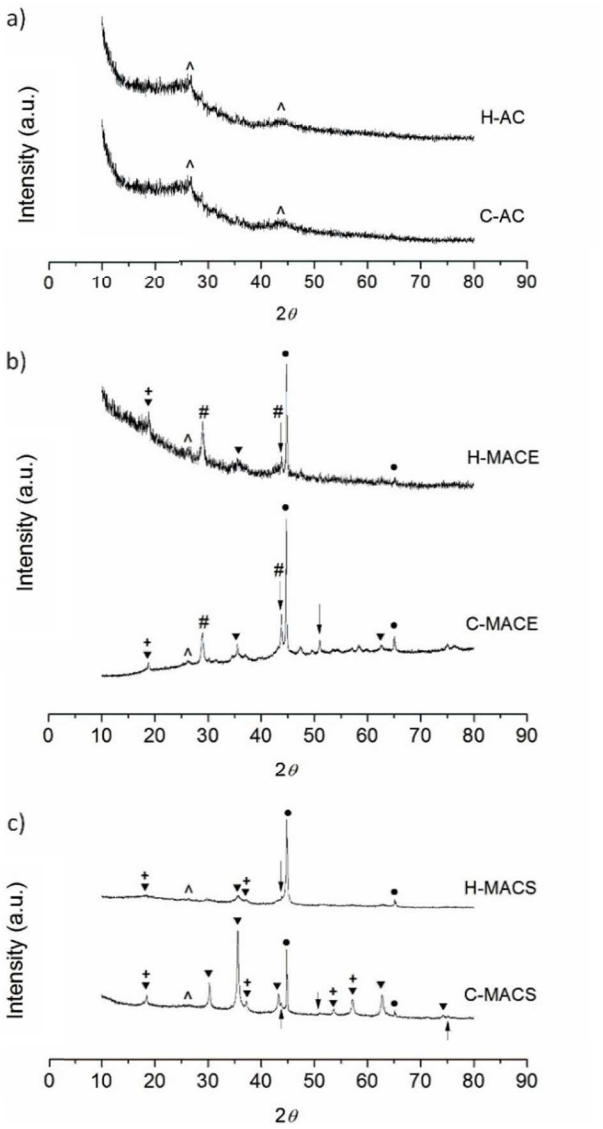

Figure 2: XRD patterns of C-AC and H-AC (a), C-MACE and H-MACE (b), C-MACS and H-MACS (c): (●) α-Fe, (^) C, (▼) Fe_3O_4, (+) MoO_2, (#) $NiMoO_4$, (↑↓) Ni_2Fe to Ni_3Fe. AC and MAC denote activated carbon and magnetic activated carbon, C-X calcined catalyst and support, H-X pre-reduced catalyst.

The XRD diffractograms of C-MACE, H-MACE, C-MACS, and H-MACS had numerous additional reflections. Well defined reflections at 2θ angles of 44.7° and 65.0° were attributed to ferrite (α-Fe; PDF: 00-006-0696) and additional characteristic reflections to magnetite (Fe_3O_4;

PDF: 00-019-0629) for all MACE and MACS samples. Furthermore, the MAC based NiMo catalysts exhibited characteristic reflections attributed to molybdenum dioxide (MoO_2; PDF: 01-086-0135) and awaruite (Ni_2Fe to Ni_3Fe; PDF: 01-088-1715). Additionally, nickel molybdenum oxide ($NiMoO_4$; PDF: 00-033-0948) was detected in C-MACE and H-MACE, but not in C-MACS and H-MACS. Note that upon pre-reducing of the C-MACS catalyst, the intensity of the Fe_3O_4 peaks reduced drastically, suggesting an α-Fe form of most iron in the H-MACS.

Mössbauer spectroscopy: Figure 3 shows the room temperature Mössbauer spectra of the C-MACE and C-MACS catalyst. In the case of the C-MACE catalyst, three different iron species are clearly identified: (i) the characteristic double sextets corresponding to the tetrahedral (A) and octahedral (B) sites of iron within magnetite, Fe_3O_4, (ii) a wide sextet with hyperfine parameters close to those corresponding to ferromagnetic bcc-Fe, and (iii) a singlet that is commonly observed in bcc-Fe(Ni) alloys with < 30 % at. of Ni content. This superparamagnetic component is attributed to the coexistence of fcc- and bcc-Fe(Ni) superparamagnetic clusters; due to fast relaxation of such magnetic clusters[30]. Most of the iron is found in the form of bcc-Fe(Ni) (66.4 at. %), although significant amounts of magnetite (17.2 at. %) and superparamagnetic Fe (16.4 at. %) are observed (Table S3).

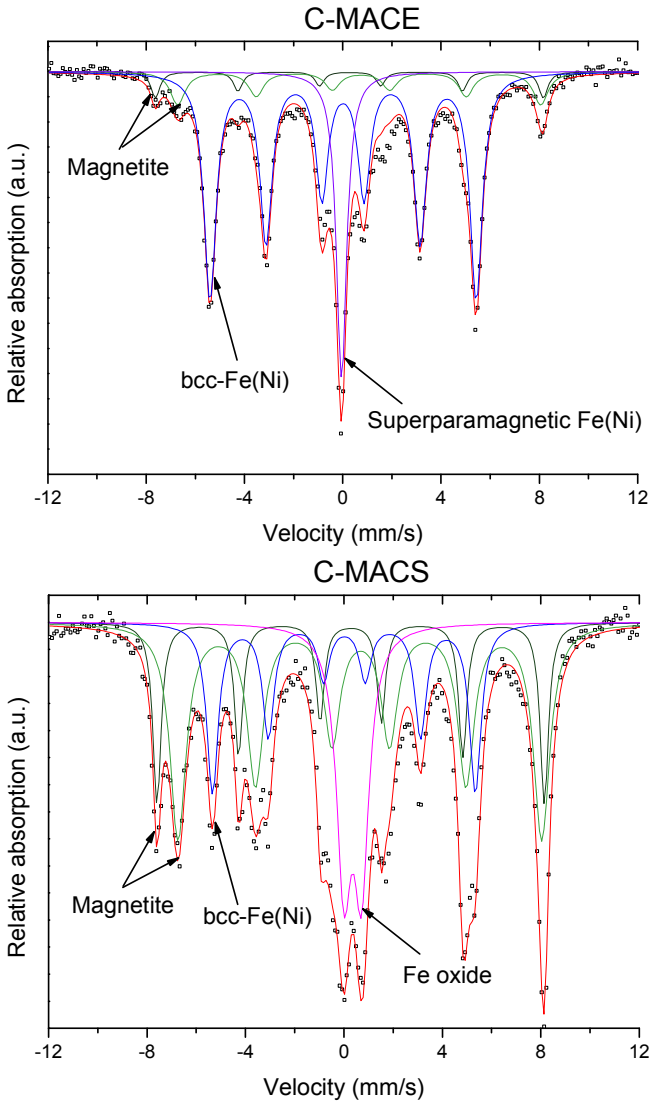

Figure 3. Room temperature Mössbauer spectra (□) for the C-MACE (up) and C-MACS (down) catalyst. The corresponding fitting (red) was done using discrete subspectra for Fe_3O_4 (green), bcc-Fe(Ni) (blue), FeO (magenta) and superparamagnetic Fe(Ni) (violet) are also shown.

In the case of the C-MACS catalysts, in addition to the magnetite and ferromagnetic bcc-Fe phases, a doublet corresponding to a paramagnetic iron oxide phase is also observed. In this case, most of the iron is in bcc-Fe form (66.4 at. %), with significant amounts of magnetite (17.2 at. %) and Ni(Fe) phase (16.4 at. %).

The unusual width of the component and the slight higher hyperfine field reveals a non-pure bcc-Fe for both C-MACE and C-MACS. It can be attributed to a substitution of Fe atoms by Ni atoms. The presence of limited quantity of magnetic Ni atoms as next neighbor in the neighborhood of the bcc-Fe atoms barely modify the hyperfine parameters of the Fe nuclei, giving as a result, similar spectral contributions which are not disclosed independently resolved and an apparent widening of the total spectrum of this phase[31]. This fact also hinders any quantization of the Ni content in this solid solution Fe(Ni) by decovolving the spectrum according with a binomial distribution of Ni atoms in the neighborhoods of the Fe atoms. However, it is clear that the bcc-Fe structure is maintained and, so, it is estimated that the Ni content remains below 30% at[32]. Conversely, there is no evidence of the presence of bimetallic FeMo in either of the catalysts: the characteristic peaks of FeMo species are not observed.

Results of catalytic conversion of lignin in a formic acid/ethanol media (LtL)

General considerations: The lignin recovery yield is given as the sum of the oil and solid yield. This value is a measure of the losses in the work-up procedure (oil and solid) together with any lignin converted to gas or non-extractable water phase compounds. Note that since the content of inorganic ashes of the rice straw lignin used for the LtL experiments was 14.9 wt.%, the solid yield given in Table 2 includes significant amounts of inorganic compounds (ashes).

The gas-phase yield refers to the fraction of all reactants that were converted into gases during the reaction, which is the sum of the gas derived from the decomposition of formic acid, gasification of ethanol and gasification of lignin. Most of the gas is accounted for by the thermal decomposition of formic acid to hydrogen and CO_2. The total decomposition of formic acid would correspond to a gas phase comprising 25 wt.% by weight of the total input for the non-

catalyzed experiments and 24.2 wt.% for the catalyzed experiments. The gasification of lignin and ethanol contribute in a lesser degree to the gas phase.

Effect of the type of bare supports: The effect of the AC, MACE and MACS bare supports on the lignin recovery yield, gas phase, oil and solid yields, and oil properties was evaluated at two different reaction conditions: 340 °C and 6 h, and 300 °C and 10 h. The data is presented in Table 2, *entries 1-8*. At 340 °C and 6 h most of the lignin was converted to either oil or solids. All the lignin recovery yields were ≥ 80 wt.%. The lower lignin recovery yields observed for the NC experiment and the AC support could be a consequence of the chemical instability of their oil components. During the work-up procedure, the oil was dewatered over solid Na_2SO_4, and the inorganic solids were eliminated by filtration. In some cases, however, the Na_2SO_4 was filtered off together with a considerable amount of organic residues. We believe that during the dewatering, unstable monomers within the oil re-polymerized, and yielded solids that were removed from the bio-oil after filtration, and thus not included in the final oil and solid yields. Thus, the NC experiment and AC support yielded more unstable oils and therefore gave lower lignin recovery yields.

Table 2: Oil yield, solid yield, gas phase, lignin recovery yield of the experiments and the elemental analysis and the average molecular weight (M_w) of the corresponding oils.

Entry	Experiment A[a]-B[b]-X[c]-Y[d]	Oil Yield[e]	Solid Yield[e]	Gas phase[f]	Lignin recovery Yield[e]	Elemental analysis Oil		M_w
						H/C	O/C	
1	NC-340-6	36.0	43.6	27.9	79.6	1.24	0.13	347
2	AC-340-6	44.4	35.7	26.6	80.1	1.35	0.15	340
3	MACE-340-6	51.0	36.7	25.6	87.7	1.23	0.13	345
4	MACS-340-6	52.3	39.1	28.3	91.4	1.28	0.13	328
5	NC-300-10	49.3	28.3	24.0	77.6	1.18	0.17	552
6	AC-300-10	50.7	30.6	22.4	81.3	1.22	0.18	483
7	MACE-300-10	49.4	40.3	23.9	89.7	1.28	0.17	412
8	MACS-300-10	50.1	43.9	25.5	94.0	1.27	0.16	381
9	C-AC-340-6	67.6	20.1	28.8	87.7	1.23	0.14	365
10	C-MACE-340-6	65.6	27.7	27.6	93.3	1.31	0.16	359
11	C-MACS-340-6	72.2	21.1	28.1	93.3	1.33	0.12	331
12	C-AC-300-10	49.2	26.2	24.0	75.4	1.23	0.20	447
13	C-MACE-300-10	63.7	34.4	23.6	98.1	1.27	0.18	444
14	C-MACS-300-10	72.0	27.7	25.6	99.7	1.27	0.18	515
15	C-Al_2O_3-300-10	50.9	26.7	24.1	77.6	1.23	0.17	431
16	C-ZrO_2-300-10	51.3	24.2	25.3	75.5	1.25	0.17	565
17	H-AC-340-6	64.9	19.6	28.7	84.5	1.24	0.14	360
18	H-MACE-340-6	61.4	27.8	27.0	89.2	1.24	0.15	439
19	H-MACS-340-6	72.8	22.7	27.2	95.5	1.29	0.13	451

[a] A: refers to the type of systems: non-supported (none), calcined catalyst (C), pre-reduced catalyst (H) [b] B: refers to the type of support: AC, MACE, MACS, Al_2O_3 (alumina) and ZrO_2 (zirconia) [c] X: Reaction temperature (°C) [d] Y: Reaction time (h) [e] The yields are given in wt.% relative to the lignin input [f] Ratio between the amount of gas produced (g) and the amount of all initial input (g)

At 340 °C and 6 h all the bare supports exhibited some catalytic activity for lignin de-polymerization, as was observed when compared with the NC system results. In the AC, MACE and MACS systems, higher oil yields coupled to lower yields of solids were obtained, as is shown in Table 2 (*entries 1-4)*, and in Figure 4 (*left)*. MACS and MACE supports also yielded higher lignin recovery yields, indicating that comparably large amount of stable oils were produced and less was lost during the work-up procedure.

GC-MS analyses of the NC, AC, MACE and MACS oils showed mostly alkyl-substituted phenols as presented in the *Supporting Information* (Table S4). Very few methoxy- or ethoxy-substituted compounds were observed. Additional intense peaks corresponding to 4-hydroxy-butanoic acid and alkyl esters were also observed. These compounds were attributed to the reaction of formic acid, ethanol and specific lignin-degradation products. An additional intense peak attributed to the product from hydrogenolysis of ethyl-phenol, 2-ethyl-1-hexanol, was also found. The main difference between the NC oil and the support only oils (AC, MACE and MACS) was that the latter contained a higher amount of alkylated phenols such as 2,3,5,6-tetramethylphenol (teMPh), 2-(1,1dimethylethyl)-3-methyl-phenol ((dME)MPh) and propofol (Prop).

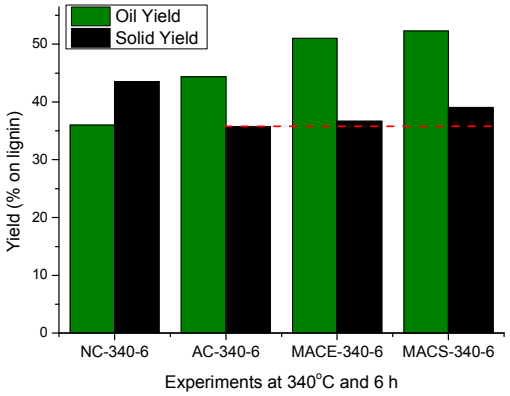

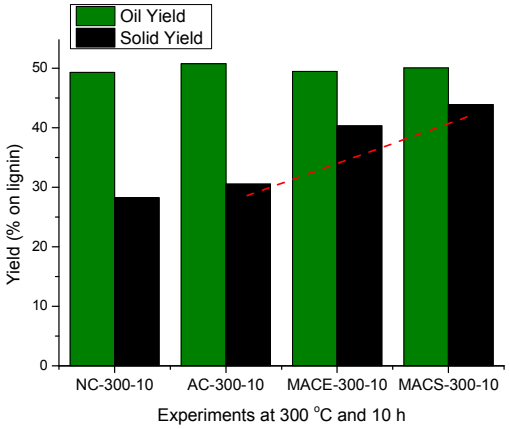

Figure 4: Oil and solid yield for the non-catalyzed and supports only experiments at 340 °C and 6 h (*left*) and at 300 °C and 10 h (*right*). AC and MAC denote activated carbon and magnetic activated carbon supports. The non-supported and catalyzed (NC) system was included for comparisons

For the experiments with the bare supports at 300 °C and 10 h, the lignin recovery yields were comparable to the ones obtained at 340 °C for 6 h. They were ~80 wt.% for the NC and AC systems and ≥90 wt.% for the MACE and MACS (*entries 5-8*, Table 2). However, no catalytic activity was observed at these reaction conditions for any of the bare supports: all the systems yielded comparable oil amounts of ~50 wt.%. The higher lignin recovery yields of the MACS and

MACE systems were due to their higher solid yields. The semi-quantitative GC-MS analysis of the oils presented in the Table S5 (Supporting information) showed relatively high concentrations of alkyl substituted guaiacols and catechols at 300 °C. Thus, the oils produced at 300°C are expected to be more unstable than the ones produced at 340°C since they contained large amounts of highly-oxygenated compounds which are known to have a higher re-polymerization tendency[33]. All the systems (NC, AC, MACE and MACS) promoted oils that contained phenol, guaiacol, ethyl phenol, ethyl benzoate ester, methyl guaiacol, ethyl guaiacol and propyl guaiacol in different concentrations.

NiMo-containing calcined catalysts (C-AC, C-MACE and C-MACS): At 340 °C and 6 h, the catalytic activities of the bare supports were considerably improved upon the addition of the Ni and Mo species. The calcined catalyst yielded higher amounts of oil and lower amounts of solids than their respective parent bare supports (*entries 1 and 9-11*, Table 2 and Figure 5, *left*). The lignin recovery yields for the C-AC, C-MACE and C-MACS were comparable, around 90 wt.%. The best results were obtained for the C-MACS catalysts with an oil yield of 72.2 wt.% and a solid yield of 21.1 wt.%. These results are comparable to the best results obtained so far with a NiMo catalyst supported on sulfated alumina: 76.5 wt. % of oil and 19.3 wt.% of solid yield[34]. This finding confirms, as already observed[34], that the type of support (i.e. activated carbon, alumina, zirconia) has a little effect on the LtL activity of the catalyst at 340 ˚C and 6 h.

The C-MACE and C-MACS catalysts yielded oils with higher H/C ratios than their C-AC and NC counterparts. The C-MACS catalyst produced the oil with the highest H/C ratio and the lowest O/C and M_w values of all the catalysts studied. The GC-MS analyses of the oils revealed that the type of catalysts (i.e. calcined catalyst or bare supports) and the type of support (AC,

MACE and MACS) did not significantly affect their compositions. Only the relative abundance of the compounds in the oils differed, as can be seen from the *Supporting Information* (Table S4).

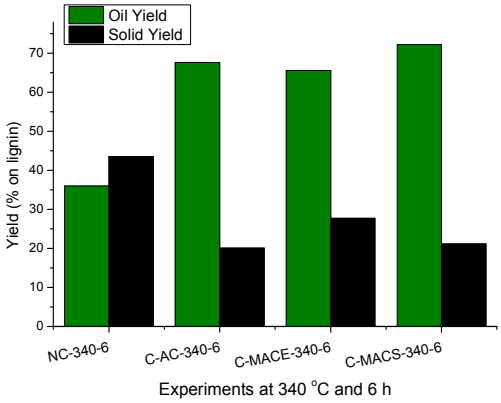

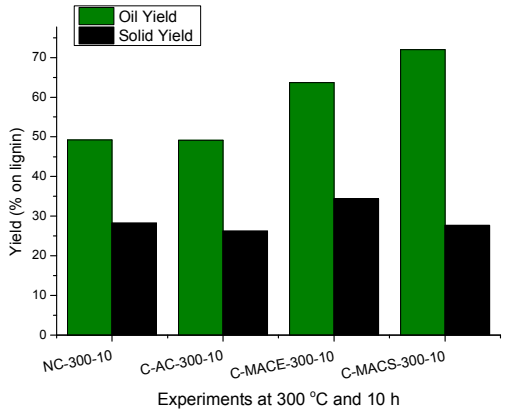

Figure 5: Oil and solid yields for the non-catalyzed and calcined catalysts (C-AC, C-MACE and C-MACS) at 340 °C and 6 h (*left*) and at 300 °C and 10 h (*right*). AC and MAC denote activated carbon and magnetic activated carbon supports. The non-catalyzed (NC) system was included for comparisons.

At 300 °C and 10 h (Figure 5), the type of support significantly affected the activity of the calcined catalysts (C-AC, C-MACE and C-MACS). For the C-MACE and C-MACS experiments,

considerably higher lignin recovery yields were obtained in comparison to the C-AC and NC systems (*entries 5 and 12-14*, Table 2). The best results were again obtained for the C-MACS catalyst with high oil yields (72.0 wt.%, the highest at this temperature) coupled with a low solid production. The C-MACE catalyst also yielded a high amount of oil (63.7 wt.%) and solids (34.4 wt.%). The C-AC, on the other hand exhibited no significant activity at this temperature of reaction, and its oil yield, solid yield and oil properties were comparable to the ones observed for the NC system. Furthermore, these catalytic activities observed for the C-MACE and C-MACS catalysts were independent of the reaction time. Additional experiments carried out at shorter reaction times, 300 ˚C and 2 h, confirmed that the C-MACE and C-MACS yielded higher lignin recovery and oil yields than the C-AC and NC systems, as is presented in the *Supporting Information* (Table S6 and Figure S1).

These results suggest that the C-MACE and C-MACS could be able to stabilize the oil components at low temperatures yielding high amount of oils after the work-up procedure. To further explore the effect of the type of support on the activity of the catalyst at 300 ˚C and 10 h, two additional experiments (*entries 15-16*, Table 2) were carried out with different calcined NiMo catalysts supported on metal oxides, i.e. C-Al_2O_3 and C-ZrO_2. The physicochemical properties of these catalysts are given elsewhere[34]. The results depicted in Figure S2 clearly showed that the C-ZrO_2 and C-Al_2O_3 catalysts exhibited no activity: the oil and solid yields obtained were comparable to the ones obtained for the NC and C-AC systems.

The higher activity towards oil stabilization observed for the C-MACE and C-MACS catalysts as compared to C-AC were confirmed when analyzing the H/C and O/C ratios of the oils. Both catalysts produced oils with a higher degree of hydrodeoxygenation (HDO) than the C-AC. The H/C ratios were higher for the C-MACE and C-MACS (1.27) as compared to the C-AC

(1.23), while their O/C ratios were slightly lower. At 300 °C and 10 h, the calcined catalysts (C-AC, C-MACE and C-MACS) and their corresponding bare supports (AC, MACE and MACS) also yielded oils with similar compositions. They contained the same type of compounds in different concentrations as can be observed from the *Supporting Information* (Table S5). The only clear difference among the calcined catalysts and the bare supports were that the oils produced with calcined catalysts contained a lower concentration of guaicols.

Pre-reduced catalysts (H-AC, H-MACE and H-MACS): Pre-reducing the catalysts did not have a significant effect in the activities of the catalysts (*entries 17-19*, Table 2). In fact, in most cases the pre-reduced catalysts exhibited lower activities than their calcined counterparts. At 340°C and 6 h, comparable oil and solid yields were obtained for the H- and C-catalysts. A graphical representation is given in the *Supporting Information* (Figure S3). Pre-reducing the catalysts had little, or even negative, effect on the properties of the oils. In the case of the H-MACE and H-MACS catalysts, lower H/C ratios, comparable O/C, and considerably higher M_w values were obtained as compared to their C-counterparts (*entries 19-20*, Table 2). The composition of the oils, measured by GC-MS, revealed that the type of compounds found in the H-series of oils were equivalent to the ones found in the C-series, as is presented in the *Supporting Information* (Table S4). The only differences were in their relative concentrations. Altogether, the GC-MS results suggested that the type of catalyst/support had a small effect on the composition of the oil, as has also been observed in related studies[34]; the reaction conditions, on the other hand, have a considerably effect on the composition of the oil.

Recycling experiments: The changes in the activity upon recycling of the C-MACS catalyst was studied for three consecutive tests at different reaction conditions and its physical and chemical

changes were monitored by ICP-EAS, SEM-EDX, N_2-adsorption and XRD. The corresponding LtL related results are summarized in Table 3.

Table 3: Oil yield, solid yield, elemental analysis and average molecular weight (M_w) of the corresponding oils for the recycling experiments

Experiment (Catalyst) A[a]-B[b]-X[c]-Y[d]	Recycling test	Oil Yield (wt.%)[e]	Solid Yield (wt.%)[e]	Elemental analysis Oil		M_w
				H/C	O/C	
C-MACS-340-6	Test (i)	72.2	21.1	1.33	0.12	331
R1-MACS-340-6	Test (ii)	56.7	37.9	1.25	0.13	326
R2-MACS-340-6	Test (iii)	47.0	42.0	1.26	0.13	304
C-MACS-300-10	Test (i)	72.0	27.7	1.27	0.18	515
R1-MACS-300-10	Test (ii)	70.6	25.8	1.27	0.19	469
R2-MACS-300-10	Test (iii)	65.0	33.4	1.29	0.20	485

[a] A: refers to the type of systems: fresh-calcined catalyst (C), recycled catalyst from the 1st cycle (R1), recycled catalyst from the 2nd cycle (R2) [b] B: refers to the type of support: AC, MACE and MACS [c] X: reaction temperature (°C) [d] Y: reaction time (h) [e] The yields are wt.% relative to the lignin input [f] Surface area of the corresponding catalyst.

At 340°C and 6 h, Figure 6 (*left*), the oil yield decreased drastically upon recycling. In the series (ii) test (the R1-MACS-340-6 experiment), the oil yield was 15.6 wt.% units lower while the solid yield was 16.8 wt.% units higher when compared with the results obtained in the series (i) test (with a fresh catalyst). In the series (iii) test (the R2-MACS-340-6 experiment), the oil yield was further decreased by 9.7 wt.% units, while the solid yield experienced a smaller increase, with 4.1 wt.% units. These trends imply that after three consecutive tests only a small amount of catalytic activity remained.

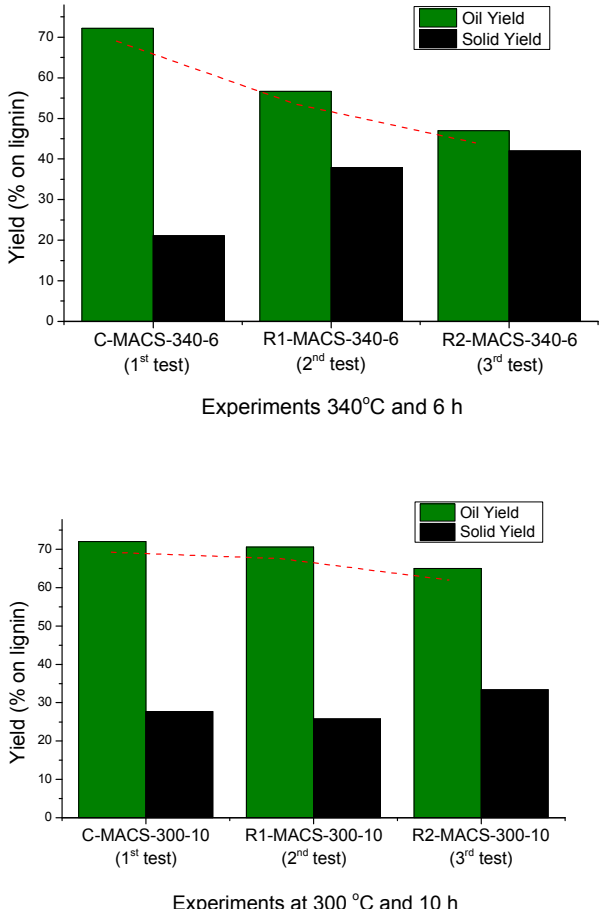

Figure 6: Oil and solid yield for the recycling experiments at 340°C and 6 h (*left*) and at 300°C and 10 h (*right*). 1st test: experiment carried out with the fresh C-MACS catalysts. 2nd test: experiments carried out with the R1-MACS-340-6 and R1-MACS-300-10. 3rd test: experiments carried out with the R2-MACS-340-6 and R2-MACS-300-10.

Table 4: BET surface area and metal content of the recycled catalysts

Experiment (Catalyst) A^a-B^b-X^c-Y^d	Recycling test	S_{BET} (m^2/g)[e]	ICP-AES			
			Ni (wt%)	Mo (wt%)	Fe (wt%)	Si (wt%)
C-MACS-340-6	1st test	1189	5.2	7.8	17.6	0.0
R1-MACS-340-6	2nd test	273	-[f]	-[f]	-[f]	-[f]
R2-MACS-340-6	3rd test	191	0.2	0.1	0.5	15.2
R1-MACS-300-10	2nd test	342	1.2	2.3	5.4	16.0
R2-MACS-300-10	3rd test	139	0.4	0.6	1.6	17.0

[a] A: refers to the type of systems: fresh-calcined catalyst (C), recycled catalyst from the 1st cycle (R1), recycled catalyst from the 2nd cycle (R2) [b] B: refers to the type of support: AC, MACE and MACS [c] X: reaction temperature (°C) [d] Y: reaction time (h) [e] Surface area of the corresponding catalyst [f] Insufficient sample amount for ICP-AES

The C-MACS catalyst underwent severe modifications upon recycling at 340°C and 6 h. The ICP-AES analysis of the R2-MACS-340-6 catalyst suggested that the C-MACS catalyst suffered from considerable metal leaching. The metal loadings for the R2-MACS-340-6 were insignificant if compared to the fresh C-MACS catalyst, with only 0.2 wt.% of Ni, 0.1 wt.% of Mo and 0.5 wt.% of Fe (Table 4). Conversely, a considerable amount of Si was incorporated on to the surface of the catalyst, as was observed by ICP-EAS and SEM-EDX (Table 4 and Figure S4 and S5). In addition, the XRD diffractogram depicted in Figure S6 (*top*) indicated that graphite and amorphous carbon phases were present on the recycled catalysts. A sharp reflection at $2\theta = 26.2°$ corresponded to graphite and a broad scattering peak of amorphous carbons at $2\theta =$ 20-30° corresponded to amorphous carbon were observed[35]. In fact, after series (ii) test, the R2-MACS-340-6 catalyst (Figure 6, *top*), displayed significant features for the graphite and amorphous carbon peaks, but minor intensities of Fe_3O_4 related reflections could be identified. All these changes were accompanied with a decreasing surface area (*c.f.* Table 4), with values

observed from 1189 m^2/g for the C-MACS, to 191 m^2/g for the R2-MACS-340-6 recovered catalyst.

A different behavior was observed when conducting the recycling tests at 300°C and 10 h (Figure 6, *right*), which suggested that the deactivation rate of the C-MACS is temperature dependent. The oil yield obtained in the series (iii) test (the R2-MACS-300-10 experiment) was only 7.0 wt.% units lower than the results in the corresponding series (i) test (fresh catalyst). A comparable increase in the solid yield, with 6.7 wt.% units, was observed. The H/C ratio was maintained at around 1.28, while the O/C ratio increased to 0.2 in the series (iii) test (*c.f.* Table 3). These trends showed that the catalytic activity of the C-MACS decreased to a lesser degree at 300 °C than at 340 °C.

At 300 °C and 10 h, the C-MACS catalyst underwent the same chemical transformations as was observed for 340 °C and 6 h. However, at 300°C and 10 h, the metal leaching was not as pronounced as in the case of the high temperature experiments. The ICP-AES analysis revealed that the metal content for the R2-MACS-300-10 catalyst was higher if compared to the R2-MACS-340-6: 0.4 wt.% of Ni, 0.6 wt.% of Mo and 1.6 wt.% of Fe (Table 4). Again, considerable amount of Si was also incorporated on the surface of the catalysts, as was observed by ICP-EAS and SEM-EDX (Table 4 and Figure S4 and S7). Graphite and amorphous carbon phases were formed upon recycling of the catalyst, as was observed by XRD (Figure S6). The surface area was reduced from 1189 m^2/g for the C-MACS, to 139 m^2/g for the R2-MACS-300-10, and the reduction was more pronounced than at high temperatures. All these findings taken together suggests that the chemical changes experienced by the catalytic surface had a stronger effect in the deactivation of the catalyst as compared to the reduction of the surface area.

DISCUSSION

In *Section 3.2.2* it was presented that the AC-340-6, MACE-340-6 and MACS-340-6 experiments rendered oils with increased concentrations of alkylated compounds and higher H/C ratios than did the NC-340-6 experiments. These findings indicate that the bare supports (AC, MACE and MACS) favored the alkylation of lignin monomers at 340 °C and 6 h. It is well stablished that alkylated lignin monomers have a lesser re-polymerization tendency than their non-alkylated counterparts[33,36], explaining the higher oil and lower solid yields observed for the AC-340-6, MACE-340-6 and MACS-340-6 experiments (*Section 3.2.2*). Such an effect was not observed, however, at a lower temperature of 300 °C and 10 h. The general affinity of ACs towards adsorption of liquid and gas components from the LtL-reaction media[37,38], and the activities of their residual acid and basic surface functionalities[39] might be behind the alkylation activity of the activated carbons. The results described in *Section 3.2.2* show that chemically similar ACs exhibited different overall catalytic properties and gave variable oil and solid yields and oil compositions.

In *Section 3.2.3*, the activities of different calcined catalysts (C-AC, C-MACE and C-MACS) containing NiMo were evaluated. The activities of bimetallic NiMo catalysts for conversion of lignin have been extensively studied by others: Ni(0) is known to catalyze the cleavage of the aryl ether bonds in lignin, while Ni promoted Mo catalysts have been proven to be active in the HDO of lignin[34] and several lignin model compounds[10,14]. However, the results of *Section 3.2.4* suggest that pre-reducing of the catalyst, and thus increasing the amount of Ni(0) species, did not increase the activity of the NiMo catalysts. Similar oil and solid yields were observed for the C-series and H-series catalyst at a temperature of 340 °C and 6 h. To study why the activity did not increase, monometallic Ni-AC and Mo-AC were synthesized following the

procedure described in the *Supporting Information* and their TPRs were compared with the ones of the C-AC and AC catalysts (Figure S8, *Supporting Information*). The TPR analysis of the Ni-AC clearly showed that below 340 °C significant amounts of the Ni^{2+} were reduced. This indicated that the Ni species could be reduced continuously during the LtL reaction under the selected experimental conditions used[34]; thus, pre-reducing of the C-AC catalyst, and therefore increasing the initial amount of Ni^0 species, did not have a significant effect in the activity of the catalyst.

The activity of the Ni and Mo phases alone were, however, temperature dependent: while at 340 °C the C-AC, C-MACE and C-MACS catalyst gave higher oil and lower solid yields than the NC counterpart. At 300 °C, the C-MACE and C-MACS gave considerably higher oil yields than the C-AC and NC experiments. The effects were independent of the reaction time. The lower activity exhibited by the C-AC at 300 °C is thought to have been a consequence of re-polymerization reactions occurring during the work-up procedure, which indicated that the C-AC oil contained a high concentration of chemically unstable products. The lack of chemical stability made it very difficult to characterize such intermediates on a molecular level, so we deduced their potential presence from the bulk oil behavior. On the other hand, the comparably high oil yields obtained for C-MACE and C-MACS suggested that they were able to produce chemically stable lignin derivatives, through HDO reactions, and thus reduce the oil loss during the work-up procedure.

The high HDO activity of the C-MACE and C-MACS catalysts at 300 °C could be related to the iron content of these catalysts. Nevertheless, this high HDO activity cannot be attributed to iron species alone: in *Section 3.2.2* it was observed that the MACE and MACS bare supports did not increase the oil yield at 300 °C and 10 h despite containing high amounts of Fe species (Table

2, *entries 5-8*). The textural properties of the ACs, the oxidation state of the Fe species or the type of support and support-acidity did not seem to affect the HDO activity of the catalyst either. First, the C-MACS catalyst had a lower surface area than the C-AC; however, the oil yield obtained for the C-MACS-300-10 experiment was significantly higher than the oil yield obtained for the C-AC-300-10 experiment. Secondly, comparable results were observed between the pre-reduced H-MACS, and the calcined C-MACS catalysts despite of containing different amounts of Fe_3O_4 and α-Fe, as were implied by the relative intensities of the corresponding XRD reflections (see *Section 3.1.3*). Thirdly, the C-AC, C-Al_2O_3 and C-ZrO_2 catalysts presented lower activity than the C-MACE and C-MACS at these reaction conditions, despite exhibiting different acidic properties.

The high HDO activity of the MAC-based catalyst could thus be attributed to the Fe-containing bimetallic species. No MoFe alloys were observed by XRD or Mössbauer spectroscopy in any of the catalysts. Thus, the characterization results described in *Section 3.1* indicate that the NiFe bimetallic species were responsible for their higher HDO activity. Resasco and co-workers claimed that NiFe catalyst supported on SiO_2 were more selective for the HDO of *m*-cresol[17] to toluene than the respective Ni and Fe monometallic catalysts. In their study, a physical mixture of Ni/SiO_2 and Fe/SiO_2 did not show this selectivity towards toluene, indicating that interactions between the two metals are important. In another study, Fang and co-workers also demonstrated that bimetallic NiFe catalysts supported on carbon nanotubes were more active towards the hydrodeoxygenation of guaiacol than mono-metallic catalysts[40]. The synergic effect of bimetallic NiFe catalysts has also been observed in other studies on the HDO of pyrolysis oils[41], simulated phenolic bio-oils[42] and even lignin depolymerization[43]. According to Resasco and co-workers[17], alloying Ni with oxophilic metals, such as Fe, weakened the interaction

between the aromatic ring and the surface, favoring a strong binding with the carbonyl group and leading to production of unsaturated compound[17,44]. This strong affinity of Fe towards oxygen will therefore favor HDO in the LtL environment, which is consistent with the findings of this study.

Lastly, the magnetic properties of C-MACS allowed it to be separated from the organic residues after the reactions. This separation allowed us to evaluate the changes of the physicochemical properties in the C-MACS catalyst and its corresponding loss of activity. The ICP-AES, EDX-SEM and XRD analyses confirmed that the catalysts underwent severe Ni, Mo and Fe leaching in the LtL reaction media. Particularly, the reduction of the Fe content in the C-MACS resulted in a loss of magnetism upon recycling. The metal leaching was more pronounced at 340 °C than at 300 °C, suggesting that the leaching is temperature dependent. This loss of magnetism limited the ease by which they could be separated from the other inorganic and organic solid fractions, as was observed by the appearance of graphite and amorphous carbon XRD signals. The appearance of graphite XRD lines could also be attributed to iron-induced graphitization[45,46].

In addition, considerable amount of Si was incorporated onto the surface of the catalysts. Note that the inorganic lignin ashes contained considerable amounts of Si (Table S7); thus, the contact between the catalyst and the inorganic lignin ashes during the LtL reaction would result in the incorporation of Si onto the catalyst surface. The N_2-adsorption monitoring of the catalyst showed that textural structure of the recovered C-MACS was severely affected by recycling. The rapidly decreasing surface area could be related to the combination of several phenomena: (*i*) the partial degradation of the MACS structure, (*ii*) the recovery of a mixture of the catalyst and organic solids with small surface areas, (*iii*) the deposition of coke and oil species on the catalytic

surface and (iv) the blocking of the pores produced by the incorporation of the Si. In any case, it appears that the textural changes of MACS were less relevant than the chemical modification of its surface chemistry as described in *Section 3.2.5*.

CONCLUSION

Two magnetic activated carbons (MACE and MACS) produced by KOH-activation of lignin-based hydrochar residues were evaluated as NiMo-catalytic supports for the LtL conversion of lignin. At 340 °C and 6 h, the highest oil yield was obtained for the C-MACS catalyst (72.2 wt.%). Moreover, the oil produced by the C-MACS catalyst at this temperature was the most upgraded: the C-MACS produced the oil with highest H/C ratio and the lowest O/C ratios and lowest M_w values. At 300 °C and 10 h, both the C-MACE and C-MACS catalysts gave considerably higher oil yields than the C-AC counterpart. It appears as the NiFe bimetallic species in the C-MACE and C-MACS increased the HDO of the bio-oil components, which in turn enhanced their stability toward re-polymerization during the work-up procedure. Hence, it leads us to conclude that iron-containing MACs are a good and suitable renewable candidate substrate to synthesize NiMo-based catalysts with outstanding HDO properties for the conversion of lignin into highly up-graded bio-oils.

In addition, the magnetism exhibited by C-MACS enabled its separation from the lignin-derived solid residues and simplified its recycling. However, loss of magnetism, leaching of the metals and incorporation of Si onto the catalyst surface are identified as important factors that cause loss of activity observed upon recycling.

ASSOCIATED CONTENT

Supporting information

Lignin ash content and its elemental characerization, synthesis of Ni-AC and Mo-AC monometallic catalysts, catalyst and bio-oil characterization procedures, lignin elemental composition and ash content, amount of reactants for every experiment, main Mössbauer parameters for the C-MACE and C-MACS catalysts , GC-MS semiquantitative analysis results, LtL results for the experiments carried out at 300 °C and 2 h, Ni, Mo, Fe and Si content of the lignin ashes, several figures comparing the oil and solid yield, SEM + EDX and XRD characterization of the C-MACS and recycled catalysts and H_2-TPR data. This material is available free of charge via the Internet at http://pubs.acs.org

AUTHOR INFORMATION

Corresponding Author

Mikel.oregui@uib.no

Author Contributions

The manuscript was written through contributions of all authors. All authors have given approval to the final version of the manuscript. ‡These authors contributed equally. (match statement to author names with a symbol)

ACKNOWLEDGEMENT

This project was supported by the Lignoref project group (including The Research Council of Norway (grant no.190965/S60), Statoil ASA, Borregaard AS, Allskog BA, Cambi AS,Xynergo

AS/Norske Skog, Hafslund ASA and Weyland AS) and by the Swedish Energy Agency and by VR and VINNOVA. The authors would also like to thank I. J. Fjellanger and Prof. I. Gandarias for their assistance in the characterization of the oil and catalysts, and the Technical College of Bergen for supplying lignin. Yulia Trushkina, and Associate Professor German Salazar-Alvarez are acknowledged for discussions and helpful input. SGIker technicaland human support (UPV/EHU, MINECO, GV/EJ, ERDF and ESF) is also gratefully acknowledged.

REFERENCE

(1) Oregui Bengoechea, M.; Hertzberg, A.; Miletić, N.; Arias, P. L.; Barth, T. Simultaneous catalytic de-polymerization and hydrodeoxygenation of lignin in water/formic acid media with Rh/Al2O3, Ru/Al2O3 and Pd/Al2O3 as bifunctional catalysts. *J Anal Appl Pyrolysis* **2015**, *113*, 713–722. DOI: 10.1016/j.jaap.2015.04.020

(2) Zakzeski, J.; Bruijnincx, P. C. A.; Jongerius, A. L.; Weckhuysen, B. M. The Catalytic Valorization of Lignin for the Production of Renewable Chemicals. *Chem Rev* **2010**, *110* (6), 3552–3599. DOI: 10.1021/cr900354u

(3) Wilson, K.; Lee, A. F. Catalyst design for biorefining. *Philos Trans R Soc London A Math Phys Eng Sci* **2016**, *374* (2061). DOI: 10.1098/rsta.2015.0081

(4) Lipinsky, E. S. Chemicals from Biomass: Petrochemical Substitution Options. *Science (80-)* **1981**, *212* (4502), 1465–1471. DOI: 10.1126/science.212.4502.1465

(5) Huang, X.; Korányi, T. I.; Boot, M. D.; Hensen, E. J. M. Catalytic Depolymerization of Lignin in Supercritical Ethanol. *ChemSusChem* **2014**, *7* (8), 2276–2288. DOI: 10.1002/cssc.201402094

(6) Haghighi Mood, S.; Hossein Golfeshan, A.; Tabatabaei, M.; Salehi Jouzani, G.; Najafi, G. H.; Gholami, M.; Ardjmand, M. Lignocellulosic biomass to bioethanol, a comprehensive review with a focus on pretreatment. *Renew Sustain Energy Rev* **2013**, *27*, 77–93. DOI: 10.1016/j.rser.2013.06.033

(7) Suhas; Carrott, P. J. M.; Ribeiro Carrott, M. M. L. Lignin – from natural adsorbent to activated carbon: A review. *Bioresour Technol* **2007**, *98* (12), 2301–2312. DOI: 10.1016/j.biortech.2006.08.008

(8) Park, Y.; Doherty, W. O. S.; Halley, P. J. Developing lignin-based resin coatings and composites. *Ind Crops Prod* **2008**, *27* (2), 163–167. DOI: 10.1016/j.indcrop.2007.07.021

(9) Jongerius, A. L.; Bruijnincx, P. C. A.; Weckhuysen, B. M. Liquid-phase reforming and hydrodeoxygenation as a two-step route to aromatics from lignin. *Green Chem* **2013**, *15* (11), 3049–3056. DOI: 10.1039/C3GC41150H

(10) Bu, Q.; Lei, H.; Zacher, A. H.; Wang, L.; Ren, S.; Liang, J.; Wei, Y.; Liu, Y.; Tang, J.; Zhang, Q.; et al. A review of catalytic hydrodeoxygenation of lignin-derived phenols from biomass pyrolysis. *Bioresour Technol* **2012**, *124*, 470–477. DOI: 10.1016/j.biortech.2012.08.089

(11) Li, B.; Lv, W.; Zhang, Q.; Wang, T.; Ma, L. Pyrolysis and catalytic pyrolysis of industrial lignins by TG-FTIR: Kinetics and products. *J Anal Appl Pyrolysis* **2014**, *108*, 295–300. DOI: 10.1016/j.jaap.2014.04.002

(12) Kleinert, M.; Barth, T. Towards a Lignincellulosic Biorefinery: Direct One-Step Conversion of Lignin to Hydrogen-Enriched Biofuel. *Energy & Fuels* **2008**, *22* (2), 1371–1379. DOI: 10.1021/ef700631w

(13) Holmelid, B.; Kleinert, M.; Barth, T. Reactivity and reaction pathways in thermochemical treatment of selected lignin-like model compounds under hydrogen rich conditions. *J Anal Appl Pyrolysis* **2012**, *98*, 37–44. DOI: 10.1016/j.jaap.2012.03.007

(14) Li, C.; Zhao, X.; Wang, A.; Huber, G. W.; Zhang, T. Catalytic Transformation of Lignin for the Production of Chemicals and Fuels. *Chem Rev* **2015**, *115* (21), 11559–11624. DOI: 10.1021/acs.chemrev.5b00155

(15) Grilc, M.; Likozar, B.; Levec, J. Simultaneous Liquefaction and Hydrodeoxygenation of Lignocellulosic Biomass over NiMo/Al2O3, Pd/Al2O3, and Zeolite Y Catalysts in

Hydrogen Donor Solvents. *ChemCatChem* **2016**, *8* (1), 180–191. DOI: 10.1002/cctc.201500840

(16) Grilc, M.; Likozar, B.; Levec, J. Kinetic model of homogeneous lignocellulosic biomass solvolysis in glycerol and imidazolium-based ionic liquids with subsequent heterogeneous hydrodeoxygenation over NiMo/Al2O3 catalyst. *Catal Today* **2015**, *256*, 302–314. DOI: 10.1016/j.cattod.2015.02.034

(17) Nie, L.; de Souza, P. M.; Noronha, F. B.; An, W.; Sooknoi, T.; Resasco, D. E. Selective conversion of m-cresol to toluene over bimetallic Ni–Fe catalysts. *J Mol Catal A Chem* **2014**, *388–389*, 47–55. DOI: 10.1016/j.molcata.2013.09.029

(18) Güvenatam, B.; Kurşun, O.; Heeres, E. H. J.; Pidko, E. A.; Hensen, E. J. M. Hydrodeoxygenation of mono- and dimeric lignin model compounds on noble metal catalysts. *Catal Today* **2014**, *233*, 83–91. DOI: 10.1016/j.cattod.2013.12.011

(19) Vissers, J. P. R.; Scheffer, B.; de Beer, V. H. J.; Moulijn, J. A.; Prins, R. Effect of the support on the structure of Mo-based hydrodesulfurization catalysts: Activated carbon versus alumina. *J Catal* **1987**, *105* (2), 277–284. DOI: 10.1016/0021-9517(87)90058-3

(20) Boorman, P. M.; Kydd, R. A.; Sorensen, T. S.; Chong, K.; Lewis, J. M.; Bell, W. S. A comparison of alumina, carbon and carbon-covered alumina as supports for Ni□Mo□F additives: gas oil hydroprocessing studies. *Fuel* **1992**, *71* (1), 87–93. DOI: 10.1016/0016-2361(92)90197-V

(21) Bailón-García, E.; Maldonado-Hódar, J. F.; Pérez-Cadenas, F. A.; Carrasco-Marín, F. Catalysts Supported on Carbon Materials for the Selective Hydrogenation of Citral. *Catalysts* **2013**, *3* (4). DOI:10.3390/catal3040853

(22) Al-Lagtah, N. M. A.; Al-Muhtaseb, A. H.; Ahmad, M. N. M.; Salameh, Y. Chemical and physical characteristics of optimal synthesised activated carbons from grass-derived sulfonated lignin versus commercial activated carbons. *Microporous Mesoporous Mater* **2016**, *225*, 504–514. DOI: 10.1016/j.micromeso.2016.01.043

(23) Rabinovich, M. L.; Fedoryak, O.; Dobele, G.; Andersone, A.; Gawdzik, B.; Lindström, M. E.; Sevastyanova, O. Carbon adsorbents from industrial hydrolysis lignin: The USSR/Eastern European experience and its importance for modern biorefineries. *Renew Sustain Energy Rev* **2016**, *57*, 1008–1024. DOI: 10.1016/j.rser.2015.12.206

(24) Ragan Neal, S. M. Activated carbon from renewable resources-lignin. *Cellul Chem Technol* **2011**, *45* (7–8), 527–531. DOI: 10.1007/978-3-319-49595-8_9

(25) Li, X.-F.; Xu, Q.; Fu, Y.; Guo, Q.-X. Preparation and characterization of activated carbon from Kraft lignin via KOH activation. *Environ Prog Sustain Energy* **2014**, *33* (2), 519–526. DOI: 10.1002/ep.11794

(26) Hao, W.; Björkman, E.; Lilliestråle, M.; Hedin, N. Activated Carbons for Water Treatment Prepared by Phosphoric Acid Activation of Hydrothermally Treated Beer Waste. *Ind Eng Chem Res* **2014**, *53* (40), 15389–15397. DOI: 10.1021/ie5004569

(27) Hao, W.; Keshavarzi, N.; Branger, A.; Bergström, L.; Hedin, N. Strong discs of activated carbons from hydrothermally carbonized beer waste. *Carbon N Y* **2014**, *78*, 521–531. DOI: 10.1016/j.carbon.2014.07.036

(28) Abioye, A. M.; Ani, F. N. Recent development in the production of activated carbon electrodes from agricultural waste biomass for supercapacitors: A review. *Renew Sustain Energy Rev* **2015**, *52*, 1282–1293. DOI: 10.1016/j.rser.2015.07.129

(29) Hao, W.; Björnerbäck, F.; Trushkina, Y.; Oregui Bengoechea, M.; Salazar-Alvarez, G.; Barth, T.; Hedin, N. High-Performance Magnetic Activated Carbon from Solid Waste from Lignin Conversion Processes. 1. Their Use As Adsorbents for CO2. *ACS Sustain*

Chem Eng **2017**, *5* (4), 3087–3095. DOI: 10.1021/acssuschemeng.6b02795

(30) Lehlooh, A.-F. D.; Mahmood, S. H. Mössbauer Spectroscopy Study of Iron Nickel Alloys. *Hyperfine Interact* **2002**, *139* (1), 387–392. DOI: 10.1023/A:1021230926166

(31) Kezrane, M.; Guittoum, A.; Hemmous, M.; Lamrani, S.; Bourzami, A.; Weber, W. Elaboration, Microstructure, and Magnetic Properties of Nanocrystalline Fe90Ni10 Powders. *J Supercond Nov Magn* **2015**, *28* (8), 2473–2481. DOI: 10.1007/s10948-015-3059-9

(32) Marcus, H. L.; Schwartz, L. H. M"ossbauer Spectra of FeMo Alloys. *Phys Rev* **1967**, *162* (2), 259–262. DOI: 10.1103/PhysRev.162.259

(33) Gasson, J. R.; Forchheim, D.; Sutter, T.; Hornung, U.; Kruse, A.; Barth, T. Modeling the Lignin Degradation Kinetics in an Ethanol/Formic Acid Solvolysis Approach. Part 1. Kinetic Model Development. *Ind Eng Chem Res* **2012**, *51* (32), 10595–10606. DOI: 10.1021/ie301487v

(34) Oregui-Bengoechea, M.; Gandarias, I.; Miletić, N.; Simonsen, S. F.; Kronstad, A.; Arias, P. L.; Barth, T. Thermocatalytic conversion of lignin in an ethanol/formic acid medium with NiMo catalysts: Role of the metal and acid sites. *Appl Catal B Environ* **2017**, *217*, 353–364. DOI: 10.1016/j.apcatb.2017.06.004

(35) Dwiatmoko, A. A.; Zhou, L.; Kim, I.; Choi, J.-W.; Suh, D. J.; Ha, J.-M. Hydrodeoxygenation of lignin-derived monomers and lignocellulose pyrolysis oil on the carbon-supported Ru catalysts. *Catal Today* **2016**, *265*, 192–198. DOI: 10.1016/j.cattod.2015.08.027

(36) Forchheim, D.; Gasson, J. R.; Hornung, U.; Kruse, A.; Barth, T. Modeling the Lignin Degradation Kinetics in a Ethanol/Formic Acid Solvolysis Approach. Part 2. Validation and Transfer to Variable Conditions. *Ind Eng Chem Res* **2012**, *51* (46), 15053–15063. DOI: 10.1021/ie3026407

(37) Franz, M.; Arafat, H. A.; Pinto, N. G. Effect of chemical surface heterogeneity on the adsorption mechanism of dissolved aromatics on activated carbon. *Carbon N Y* **2000**, *38* (13), 1807–1819. DOI: 10.1016/S0008-6223(00)00012-9

(38) Li, B.; Lei, Z.; Huang, Z. Surface-Treated Activated Carbon for Removal of Aromatic Compounds from Water. *Chem Eng Technol* **2009**, *32* (5), 763–770. DOI: 10.1002/ceat.200800535

(39) Rodríguez-reinoso, F. The role of carbon materials in heterogeneous catalysis. *Carbon N Y* **1998**, *36* (3), 159–175. DOI: 10.1016/S0008-6223(97)00173-5

(40) Fang, H.; Zheng, J.; Luo, X.; Du, J.; Roldan, A.; Leoni, S.; Yuan, Y. Product tunable behavior of carbon nanotubes-supported Ni–Fe catalysts for guaiacol hydrodeoxygenation. *Appl Catal A Gen* **2017**, *529*, 20–31. DOI: 10.1016/j.apcata.2016.10.011

(41) Leng, S.; Wang, X.; He, X.; Liu, L.; Liu, Y.; Zhong, X.; Zhuang, G.; Wang, J. NiFe/γ-Al2O3: A universal catalyst for the hydrodeoxygenation of bio-oil and its model compounds. *Catal Commun* **2013**, *41*, 34–37. DOI: 10.1016/j.catcom.2013.06.037

(42) Shafaghat, H.; Rezaei, P. S.; Daud, W. M. A. W. Catalytic hydrodeoxygenation of simulated phenolic bio-oil to cycloalkanes and aromatic hydrocarbons over bifunctional metal/acid catalysts of Ni/HBeta, Fe/HBeta and NiFe/HBeta. *J Ind Eng Chem* **2016**, *35*, 268–276. DOI: 10.1016/j.jiec.2016.01.001

(43) Zhai, Y.; Li, C.; Xu, G.; Ma, Y.; Liu, X.; Zhang, Y. Depolymerization of lignin via a non-precious Ni-Fe alloy catalyst supported on activated carbon. *Green Chem* **2017**, *19* (8), 1895–1903. DOI: 10.1039/C7GC00149E

(44) Robinson, A. M.; Hensley, J. E.; Medlin, J. W. Bifunctional Catalysts for Upgrading of

Biomass-Derived Oxygenates: A Review. *ACS Catal* **2016**, 5026–5043. DOI: 10.1021/acscatal.6b00923

(45) Baraniecki, C.; Pinchbeck, P. H.; Pickering, F. B. Some aspects of graphitization induced by iron and ferro-silicon additions. *Carbon N Y* **1969**, *7* (2), 213–224. DOI: 10.1016/0008-6223(69)90104-3

(46) Weisweiler, W.; Subramanian, N.; Terwiesch, B. Catalytic influence of metal melts on the graphitization of monolithic glasslike carbon. *Carbon N Y* **1971**, *9* (6), 755–761. DOI: 10.1016/0008-6223(71)90008-X

TABLE OF CONTENTS (TOC) GRAPHIC

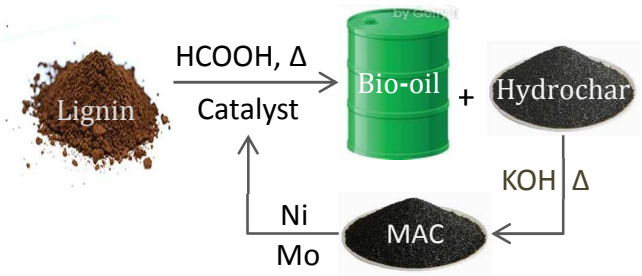

Synopsis: lignin conversion processes generates large quantities of hydrochar. This sub-product can be valorized into magnetic activated carbon and re-used as catalyst support.

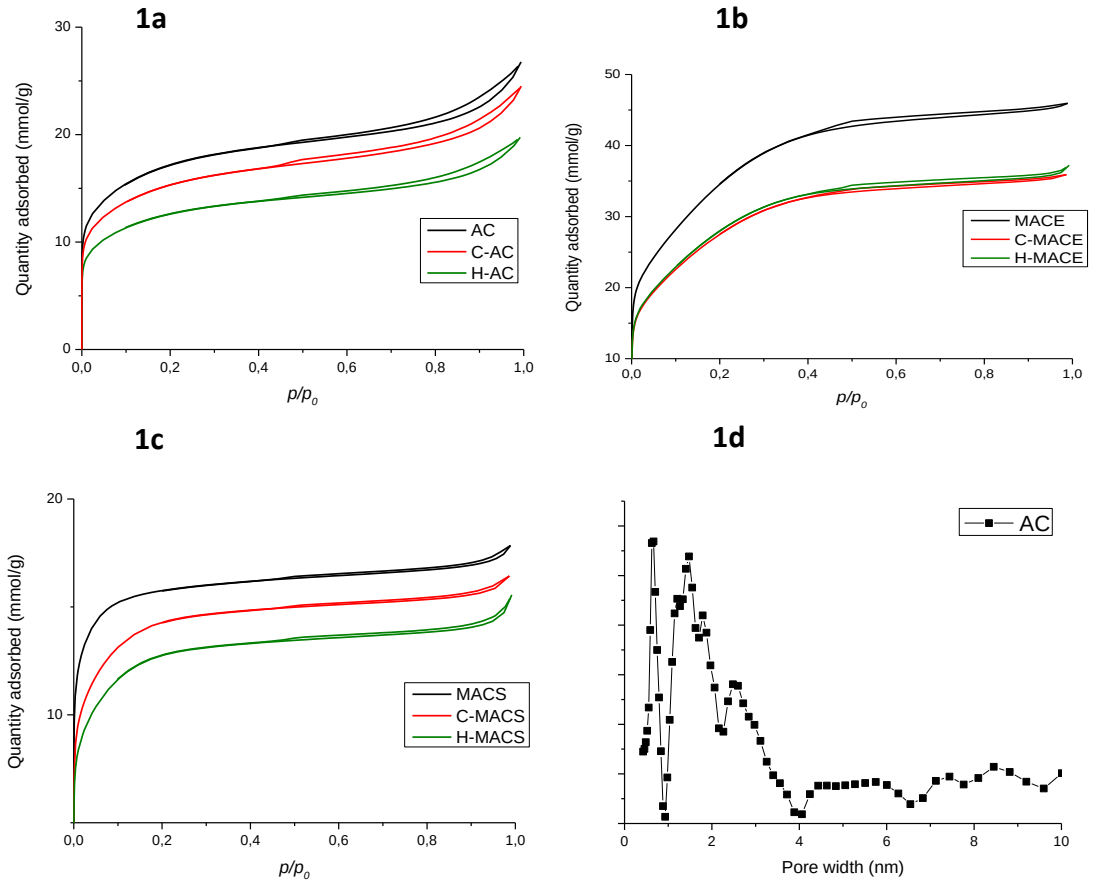

Figure 1. N_2 adsorption-desorption isotherms for: (a) AC (black), C-AC (red) and H-AC (green); (b) MACE (black), C-MACE (red) and H-MACE (green); (c) MACS (black), C-MACS (red) and H-MACS (green). MAC denotes magnetic activated carbon, C-X NiMo containing calcined catalyst and support, H-X NiMo containing pre-reduced catalyst. The N_2 isotherms for MACE and MACS are reported elsewhere[29] (d) pore size distribution for the AC carbon using DFT model

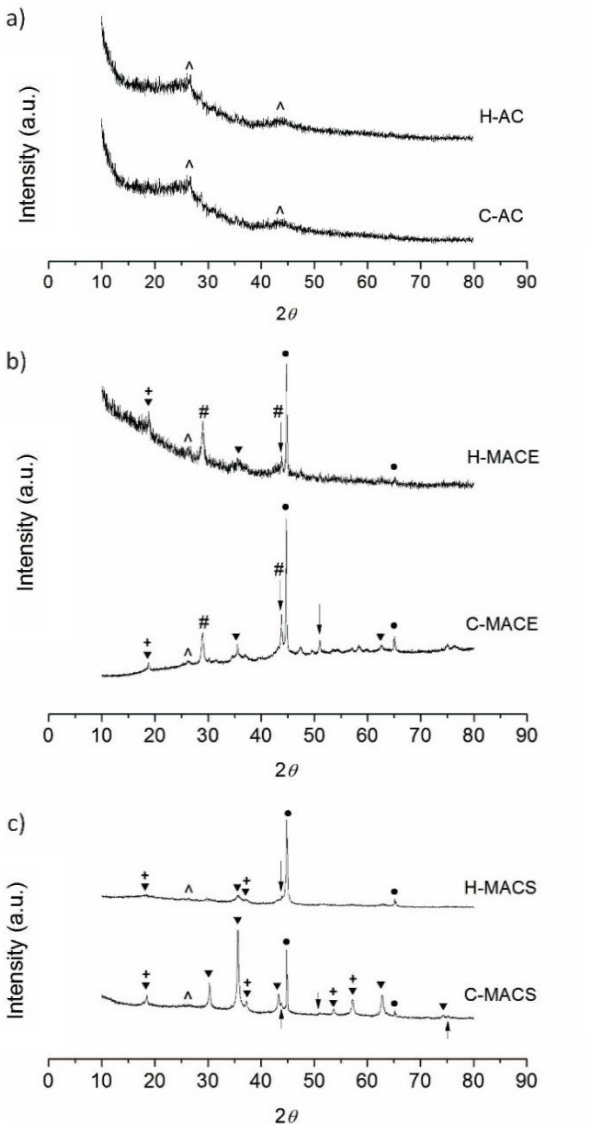

Figure 2. XRD patterns of C-AC and H-AC (a), C-MACE and H-MACE (b), C-MACS and H-MACS (c): (●) α-Fe, (^) C, (▼) Fe_3O_4, (+) MoO_2, (#) $NiMoO_4$, (↑↓) Ni_2Fe to Ni_3Fe. AC and MAC denote activated carbon and magnetic activated carbon, C-X calcined catalyst and support, H-X pre-reduced catalyst.

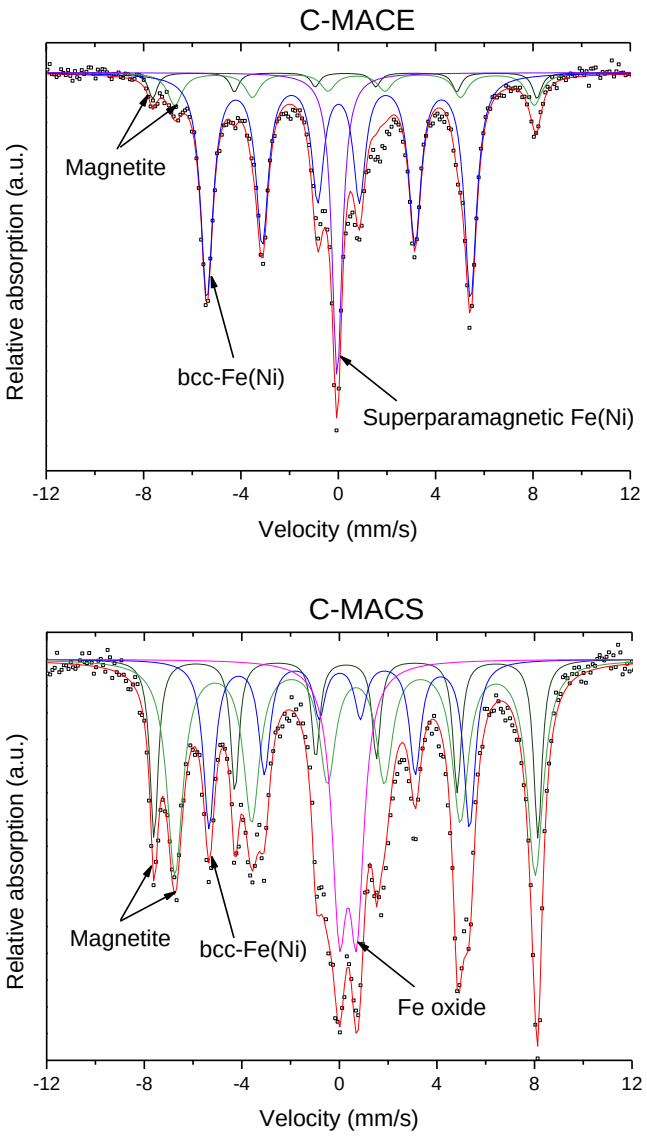

Figure 3. Room temperature Mössbauer spectra (□) for the C-MACE (up) and C-MACS (down) catalyst. The corresponding fitting (red) was done using discrete subspectra for Fe_3O_4 (green), bcc-Fe(Ni) (blue), FeO (magenta) and superparamagnetic Fe(Ni) (violet) are also shown.

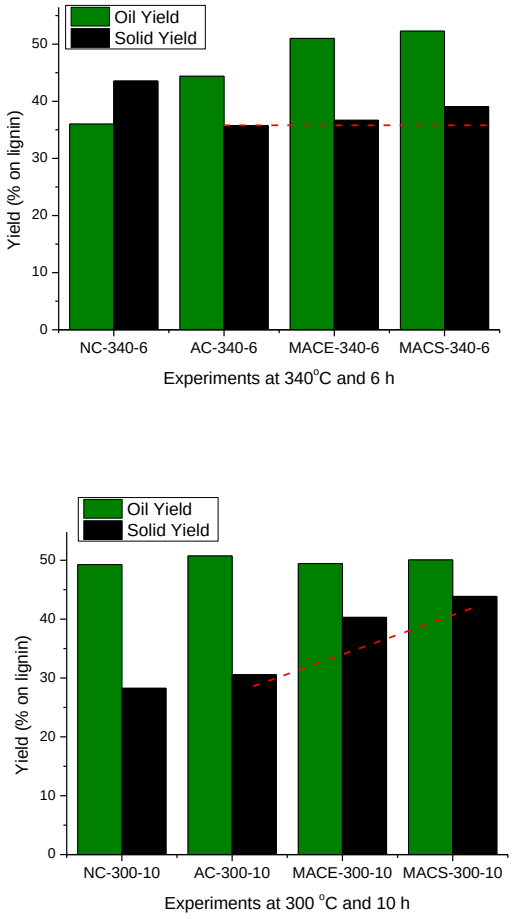

Figure 4: Oil and solid yield for the non-catalyzed and supports only experiments at 340 °C and 6 h (*left*) and at 300 °C and 10 h (*right*). AC and MAC denote activated carbon and magnetic activated carbon supports. The non-supported and catalyzed (NC) system was included for comparisons.

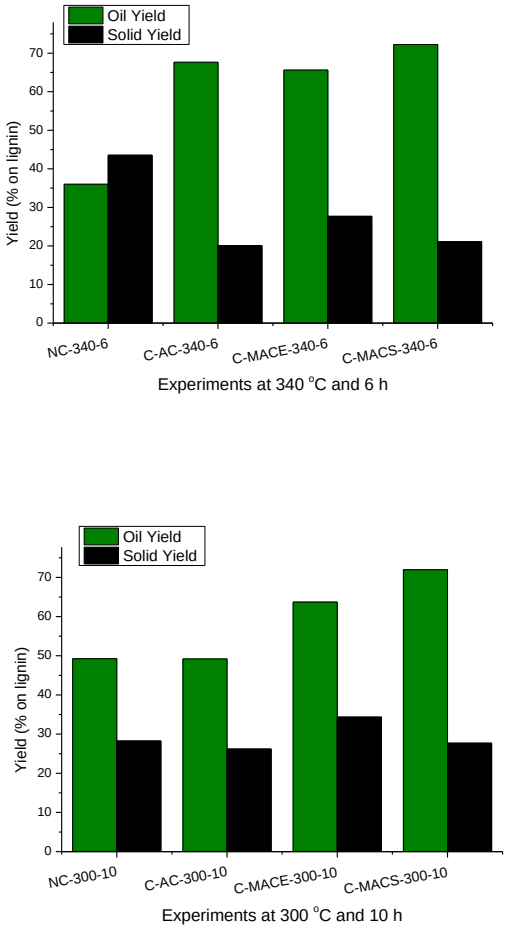

Figure 5: Oil and solid yields for the non-catalyzed and calcined catalysts (C-AC, C-MACE and C-MACS) at 340 °C and 6 h (*left*) and at 300 °C and 10 h (*right*). AC and MAC denote activated carbon and magnetic activated carbon supports. The non-catalyzed (NC) system was included for comparisons.

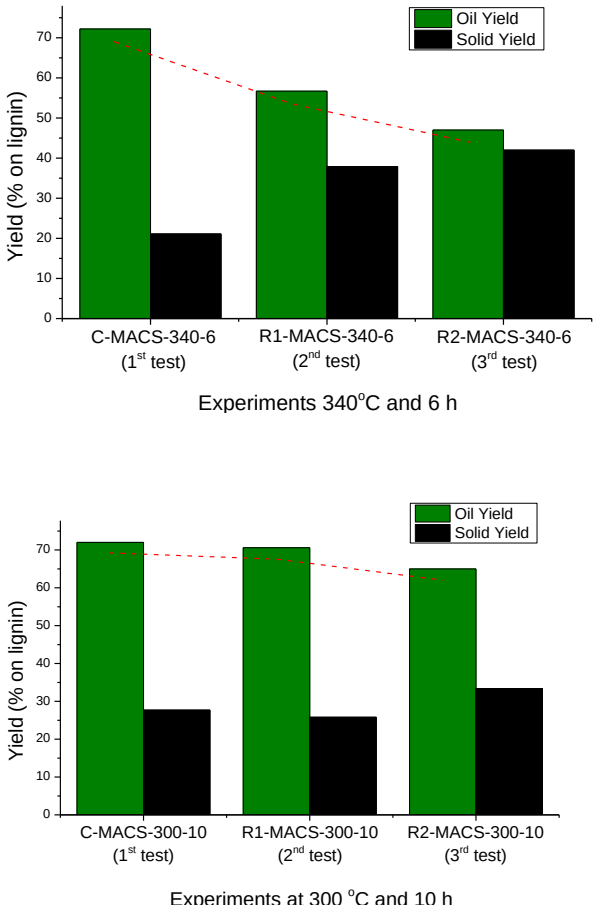

Figure 6: Oil and solid yield for the recycling experiments at 340°C and 6 h (*left*) and at 300°C and 10 h (*right*). 1st test: experiment carried out with the fresh C-MACS catalysts. 2nd test: experiments carried out with the R1-MACS-340-6 and R1-MACS-300-10. 3rd test: experiments carried out with the R2-MACS-340-6 and R2-MACS-300-10.